Molecular Biology of the Cell
Vol. 9, 237–247, February 1998

Evidence for Four Cytoplasmic Dynein Heavy Chain Isoforms in Rat Testis

Peggy S. Criswell and David J. Asai*

Department of Biological Sciences, Purdue University, West Lafayette, Indiana, 47907-1392

Submitted September 29, 1997; Accepted November 19, 1997
Monitoring Editor: Paul Matsudaira

Recent studies have revealed the expression of multiple putative cytoplasmic dynein heavy chain (DHC) genes in several organisms, with each gene encoding a separate protein isoform. This finding is consistent with the hypothesis that different isoforms do different things, as is the case for the axonemal dyneins. Furthermore, the large number of tasks ascribed to cytoplasmic dynein suggests that there may be additional isoforms not yet identified. Two of the mammalian cytoplasmic dynein heavy chains are DHC1a and DHC1b. DHC1a is conventional cytoplasmic dynein and is found in all organisms examined. DHC1b is expressed in organisms that have multiple dyneins, and has been implicated in the intracellular trafficking of molecules in unciliated and ciliated cells. In the present study, we examined the DHC1b protein from rat testis. Testis cytoplasmic dynein contains a large amount of dynein heavy chain reactive with an antibody raised against a peptide sequence of rat DHC1b. The testis anti-DHC1b immunoreactive protein is slightly smaller than testis DHC1a, as assessed by SDS-PAGE. In Northern blots, the DHC1b mRNA is smaller than the DHC1a mRNA. In sucrose gradients made in low ionic strength, DHC1a sedimented at approximately 20S, and the anti-1b immunoreactive heavy chains sedimented in a broad band centered at approximately 14S. The V1-photolysis reaction of individual sucrose gradient fractions revealed three distinct patterns of photolysis, suggesting that there are at least three separate 1b-like heavy chain isoforms in testis. Using a high-stringency Western blotting protocol, the anti-1b antibody and the anti-DHC2 antibody recognized the same heavy chain and specifically bound to one of the three 1b-like heavy chains. We conclude that rat testis contains three 1b-like dynein heavy chains, and one of these is the product of the DHC1b/DHC2 gene previously identified.

INTRODUCTION

The dyneins are the family of high molecular weight (M_r) motor proteins that produce directed movement along microtubules (recently reviewed in Holzbaur and Vallee, 1994; Mitchell, 1994; Porter, 1996). The dynein family is divided into two functional classes: axonemal dynein, which produces the active sliding between outer doublet microtubules that underlies the propagated bending of cilia and flagella (Satir, 1965; Summers and Gibbons, 1971); and cytoplasmic dynein, which participates in numerous cellular activities (summarized in Collins, 1994). Within the dynein complex, the dynein heavy chain (DHC, M_r >500,000) is the actual motor, possessing the Mg-ATPase and ATP-sensitive microtubule-binding activities (Sale and Fox, 1988; Mazumdar *et al.*, 1996).

Many organisms use multiple dynein heavy chain isoforms that are the products of multiple DHC genes (reviewed in Asai, 1996). In our studies, we have adopted the nomenclature of Gibbons (1995), which is based on patterns of sequence similarities in the central catalytic domain, to describe the DHC family. For the axonemal class of dyneins, the current view is that specific combinations of the approximately 12 heavy chain isoforms are precisely located within the axoneme, where they produce distinct forces that are integrated to generate the overall pattern of ciliary bend-

* Corresponding author.

ing (Piperno and Ramanis, 1991; Smith and Sale, 1992; reviewed in Asai and Brokaw, 1993; Brokaw, 1994). In contrast to the axonemal dyneins, much less is known about the extent of the diversity of cytoplasmic heavy chain isoforms and how that diversity may be related to function.

Cytoplasmic (i.e., nonaxonemal) dynein has been implicated in a wide array of tasks including: retrograde fast axonal transport of organelles and vesicles (Schnapp and Reese, 1989; Schroer *et al.*, 1989; Muresan *et al.*, 1996) and slow axonal transport of microtubules (Cleveland and Hoffman, 1991; Dillman *et al.*, 1996); positioning of intracellular organelles, including the secretory apparatus (Corthesy-Theulaz *et al.*, 1992; Aniento *et al.*, 1993; Fath *et al.*, 1994; Oda *et al.*, 1995; Holleran *et al.*, 1996); the organization of the microtubule cytoskeleton in interphase cells (Koonce and Samso, 1996); nuclear positioning (Eshel *et al.*, 1993; Li *et al.*, 1993; Plamann *et al.*, 1994; Xiang *et al.*, 1994); and the assembly and separation of the mitotic apparatus (Pfarr *et al.*, 1990; Steuer *et al.*, 1990; Verde *et al.*, 1991; Vaisberg *et al.*, 1993; Saunders *et al.*, 1995; Echeverri *et al.*, 1996). This wide diversity of tasks and force requirements (e.g., fast versus slow axonal transport) represents an obvious opportunity to exploit multiple cytoplasmic isoforms. However, until recently only a single cytoplasmic dynein heavy chain had been characterized. This conventional cytoplasmic dynein, herein called DHC1a, is present in all eukaryotes and forms a two-headed homodimer (Vallee *et al.*, 1988; Neely *et al.*, 1990). In budding yeast, filamentous fungi, and slime mold, DHC1a is apparently the only dynein expressed, demonstrating that other dynein isoforms are not required in these organisms.

Recent studies in other model organisms compel a reevaluation of the diversity of cytoplasmic dynein (Gibbons *et al.*, 1994; Tanaka *et al.*, 1995). In both unciliated and ciliated mammalian cells, there are multiple cytoplasmic dynein heavy chain isoforms that appear to perform separate tasks. Three isoforms were characterized in fibroblasts (Vaisberg *et al.*, 1996): DHC1, which is the same as DHC1a, is conventional cytoplasmic dynein; DHC2, which is the same as DHC1b, is involved in positioning the Golgi apparatus; and DHC3 is associated with what may be transport intermediates between intracellular compartments. In ciliated tracheal cells, DHC1a and DHC1b were shown to have distinct patterns of expression and location, implying that they perform separate functions (Criswell *et al.*, 1996). The identification of new isoforms of cytoplasmic dynein that are located in specific places in the cell supports the hypothesis that the cytoplasmic dyneins, like the axonemal isoforms, are functionally specialized. Thus far, only a few different cytoplasmic DHC isoforms have been identified. However, if the cytoplasmic dyneins are specialized, then perhaps there are additional isoforms not yet discovered that are used to perform the many tasks assigned to cytoplasmic dynein.

Rat testis has previously been shown to be a rich source of cytoplasmic dynein (Collins and Vallee, 1989; Neely *et al.*, 1990; Hall *et al.*, 1992). Testis cytoplasmic dynein contains a large amount of dynein heavy chain that is immunoreactive with an antibody raised against a peptide sequence derived from DHC1b. With the hope that testis might be a good source from which to purify large quantities of the DHC1b isoform, we characterized this material further. The DHC1a and the heavy chains that were immunoreactive with anti-DHC1b were separated in sucrose gradients. Vanadate-mediated photolysis and Western blotting experiments indicated that there are at least three distinct heavy chain isoforms in addition to DHC1a. One of these three is the gene product of DHC1b/2. The other two may represent novel cytoplasmic dynein isoforms.

MATERIALS AND METHODS

Cytoplasmic Dynein Isolation

Cytoplasmic dynein was prepared using standard methods (Amos, 1989). Testes were removed from asphyxiated adult Sprague Dawley rats and rinsed in phosphate-buffered saline (PBS) before decapsulation. The decapsulated tissue was homogenized in one volume of homogenization buffer: 0.1 M [piperazine-*N,N′*-bis(2-ethanesulfonic acid)disodium salt] (PIPES), 2 mM $MgSO_4$, 1 mM [ethylene glycol bis(β-aminoethyl ether) *N,N,N′N′*-tetra-acetic acid] (EGTA), 0.5 mM dithiothreitol, and 4 M glycerol supplemented with the protease inhibitors phenylmethylsulfonyl fluoride (0.3 mM), *Nα-p*-Tosyl-L-arginine methyl ether (1 mM), pepstatin A (2 μg/ml), leupeptin (2 μg/ml, aprotinin (2 μg/ml), and soybean trypsin inhibitor (100 μg/ml). The homogenate was clarified at 30,000 × *g* for 45 min at 4°C and centrifuged again at 160,000 × *g* for 2 h at 4°C. Taxol (Calbiochem, La Jolla, CA) was added at a final concentration of 20 μM to the high-speed supernatant to induce microtubule polymerization. The microtubules were sedimented through a 10% sucrose cushion and washed twice in homogenization buffer without glycerol. The dynein was eluted from the microtubules in wash buffer (0.1 M PIPES, 8 mM $MgSO_4$, 1 mM EDTA) supplemented with either 0.5 M NaCl or 10 mM ATP, as noted in the text. Although the overall protein compositions of the two extracts were different, the cytoplasmic dynein heavy chains from both preparations behaved in the same manner in these experiments.

Northern Blotting

Total RNA was obtained from adult Sprague Dawley rat testes using guanidinium thiocyanate (Chomczynski and Sacchi, 1987). Poly(A)$^+$ RNA was isolated with an oligo-dT kit (Pharmacia LKB Biotech, Piscataway, NJ). Approximately 20 μg of poly(A)$^+$ RNA were electrophoresed in a 0.8% agarose/formaldehyde gel (Sambrook *et al.*, 1989) and transferred by capillary action to Genescreen Plus membrane (New England Nuclear Research Products, Boston, MA). Northern blots were hybridized with the 300-bp fragments of DHC1a and DHC1b as described previously (Criswell *et al.*, 1996). Blots were washed in 100 mM sodium phosphate at 50°C for 30 min (low-stringency wash, Figure 2A), and in 50 mM sodium phosphate at 65°C for 30 min (high-stringency wash, Figure 2B). The specific activities of the DHC1a and DHC1b probes were 7.3×10^8 cpm/ng and 3.0×10^9 cpm/ng, respectively.

Sucrose Density Gradient Centrifugation

The preparations of cytoplasmic dynein were sedimented in 10-ml, linear 5–20% sucrose gradients made in wash buffer with 0.5 M NaCl (high ionic strength) and without the added NaCl (low ionic strength). The gradients were centrifuged in a Beckman SW41 rotor at 35,000 rpm for 16 h at 4°C. The standards catalase (11.3S) and thyroglobulin (19.2S) were sedimented in parallel gradients. Following centrifugation, the gradients were divided into 30 equal-volume fractions.

ATPase assays of the fractions were performed using our standard methods (Asai and Wilson, 1985). Liberated phosphate was measured using the malachite green method (Carter and Karl, 1982).

SDS-PAGE and Western Blotting

Proteins were electrophoresed in 6.7% Laemmli (Laemmli, 1970) gels or in 8% Dreyfuss (Dreyfuss *et al.*, 1984) gels (Figure 4 only). Gels were stained with silver (Merril *et al.*, 1981). Following electrophoresis, the protein samples were transferred onto nitrocellulose and probed with antibodies. Anti-1a and anti-1b are rabbit antibodies raised against synthetic peptides derived from rat DHC1a and DHC1b and affinity purified with the appropriate peptide (Criswell *et al.*, 1996). The anti-DHC2 antiserum was a generous gift from Eugeni Vaisberg (University of Colorado, Boulder, CO). The pan-reactive anti-cytoplasmic dynein antibody JR is a rabbit antiserum raised against the DHC P1-loop sequence that is present in both DHC1a and DHC1b (Asai *et al.*, 1994). The monoclonal antibody raised against intermediate chain IC74 (Dillman and Pfister, 1994) was obtained from Chemicon International (Temecula, CA). Peroxidase-conjugated secondary antibodies were donkey anti-rabbit IgG (Amersham, Arlington Heights, IL) and goat anti-mouse IgG (Kirkegaard and Perry, Gaithersburg, MD). Western blots were developed with Super Signal substrate (Pierce, Rockford, IL) and exposed to x-ray film. In this study, two protocols were used to prepare the blots. The low-stringency conditions were similar to what we described previously (Criswell *et al.*, 1996), in which the blots were washed three times in Tris-buffered saline supplemented with 0.25% Tween 20 (TBST) between and after antibody incubations. The high-stringency conditions first treated the blots in stripping solution (62.5 mM Tris, pH 6.8, 100 mM 2-mercaptoethanol, 2% SDS, incubated at 50°C for 30 min) and washed the blots 6–12 times in TBST between and after antibody incubations.

V1 Photolysis of Dynein

The V1-photolysis conditions were: 1 mM $MgATP^{2-}$, 200 μM sodium orthovanadate, and irradiation at 365 nm on ice for 1.5 h. After irradiation, the samples were mixed with 5× Laemmli SDS-PAGE sample buffer, heated at 95°C for 10 min, and stored at −20°C until electrophoresis.

Preparation of Figures

The figures of the silver-stained gels, the autoradiograms, and the chemiluminescence Western blots were produced by digitizing the raw data on a flatbed scanner, importing the images into PowerPoint (Microsoft, Seattle, WA) where they were trimmed and lettered, and printing the file. The images were not otherwise modified. Care was taken to allow for an objective comparison of results. In multi-panel figures, the various sections came from the same gel or x-ray film and were thus stained or exposed identically, and the sections were scanned identically. In cases where the sucrose gradient fractions needed to be accommodated in two gels, the gels were run side by side, stained together, and scanned together.

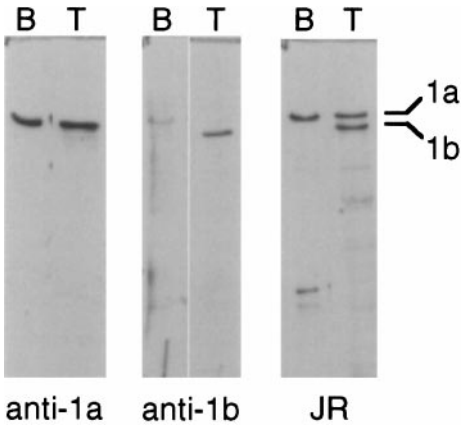

Figure 1. Western blots of cytoplasmic dyneins from rat brain and testis. Three identical blots containing cytoplasmic dyneins isolated from rat brain (B) and rat testis (T) were resolved by 6.7% SDS-PAGE, transferred to nitrocellulose, and probed with antibodies to DHC1a (anti-1a) and DHC1b (anti-1b) and with the pan-reactive anticytoplasmic dynein antibody (JR). Blots were developed with horseradish peroxidase–conjugated secondary antibodies, followed by chemiluminescence and exposure to x-ray film. The anti-1b-immunoreactive protein from testis, but not brain, was smaller than DHC1a.

RESULTS

Anti-1b Immunoreactive Protein Is Abundant in Rat Testis and Is Slightly Smaller than DHC1a

Preparations of crude cytoplasmic dyneins obtained from rat brain and rat testis were examined by Western blotting (Figure 1). The blots were probed with the previously characterized antibodies raised against synthetic peptides from rat DHC1a and DHC1b and with the pan-reactive antibody to cytoplasmic dynein, JR. The anti-1a antiserum recognized a polypeptide of approximately M_r 500,000 in both brain and testis samples (Figure 1, left blot). The anti-1b antiserum very weakly stained a band of the same size as that of the DHC1a in the brain sample, and more strongly stained a slightly smaller polypeptide in the testis sample (Figure 1, middle blot). The HMr brain dynein band and the two bands from testis reacted with the JR antiserum (Figure 1, right blot). On the basis of their relative migrations in the gels, the anti-1b-immunoreactive polypeptide from testis was estimated to be approximately 60 kDa smaller than DHC1a from brain and testis. In addition to the difference in sizes, a significantly greater quantity of the anti-1b immunoreactive protein was present in the testis sample than in the brain sample, as illustrated in the middle blot in Figure 1. Because each pair of samples in the blots shown in Figure 1 were electrophoresed side by side and were probed and developed identically, the relative quantities of the two proteins can be estimated from this figure. We conclude that the anti-1a- and anti-1b-immunoreactive proteins from testis, but not

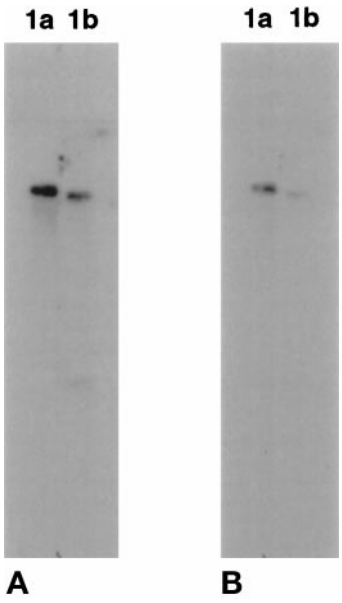

Figure 2. Northern blots of rat testis RNA. Twenty micrograms of testis poly(A)$^+$ RNA were resolved on a 0.8% agarose gel under denaturing conditions. Samples were blotted onto membranes and hybridized overnight with ^{32}P-labeled 300-bp cDNA probes derived from DHC1a and DHC1b. Identical strips were individually probed with one of the cDNAs, and the strips were exposed side by side to the x-ray film. (A) Autoradiogram after low-stringency wash (100 mM sodium phosphate, 50°C). (B) Autoradiogram of the same blots after high-stringency wash (50 mM sodium phosphate, 65°C). The DHC1b transcript is smaller and appears to be less abundant than the DHC1a mRNA.

from brain, can be resolved by SDS-PAGE. Furthermore, relative to brain, the testis is enriched in anti-1b-immunoreactive protein.

DHC1b mRNA Is Slightly Smaller than DHC1a mRNA from Testis

In our previous study, Northern blots showed that DHC1a and DHC1b mRNAs from rat brain are the same size (Criswell *et al.*, 1996). Using the same cDNA probes, we evaluated the expression of DHC1a and DHC1b mRNAs in rat testis. Northern blots of testis poly(A)$^+$ RNA resolved in a 0.8% denaturing gel indicated that DHC1a mRNA is slightly larger than DHC1b (Figure 2). Single bands representing DHC1a and DHC1b mRNAs (approximately 15 kb) were detected on the blot after washes at low stringency (100 mM sodium phosphate, 50°C, Figure 2A). After a higher stringency wash (50 mM sodium phosphate, 65°C; Figure 2B), the intensities of both bands diminished, but the relative ratio between the two bands did not change significantly. We conclude that DHC1b mRNA is slightly smaller and less abundant than DHC1a mRNA in rat testis.

DHC1a and DHC1b Can Be Separated in Sucrose Gradients

The Western blots of testis dyneins (summarized in Figure 1) indicated that anti-1a- and anti-1b-immunoreactive proteins are resolved by SDS-PAGE. We took advantage of this apparent size difference to evaluate the sedimentation patterns of the dyneins in sucrose gradients. A 0.5 M NaCl extract from Taxol-induced cytoplasmic microtubules was sedimented through a 5–20% linear sucrose gradient made in low ionic strength, the gradient was divided into 30 equal-volume fractions, and the fractions were analyzed by SDS-PAGE (Figure 3). Low-stringency Western blots of the gradient fractions revealed that the anti-1a-immunoreactive protein sedimented with a velocity centered at approximately 20S, and the anti-1b-immunoreactive protein sedimented with a velocity centered at approximately 14S. The gradient fractions were analyzed for Mg-ATPase activity (Figure 3). Two broad peaks of activity corresponding to the presence of the dynein heavy chains were observed. In other experiments, fractions enriched in DHC1a and in DHC1b were separately pooled, dialyzed into low-ionic strength buffer, and resedimented through fresh 5–20% sucrose gradients. The two dyneins resedimented appropriately: DHC1a again centered at approximately 20S and DHC1b centered at approximately 14S. A M_r 74,000 polypeptide was observed to cosediment with DHC1a but not with DHC1b.

Dynein Intermediate Chain IC74 Associates with DHC1a But Not with the Anti-1b-Immunoreactive Protein

To determine whether the M_r 74,000 polypeptide that cosedimented with DHC1a was the cytoplasmic dynein intermediate chain IC74, a Western blot experiment was performed. Samples from a sucrose gradient similar to the one shown in Figure 3 were electrophoresed, transferred to nitrocellulose, and probed with the anti-IC74 antibody (Figure 4). In this gradient, DHC1a sedimented in fractions 17–23, with its peak of concentration in fractions 19–21, and DHC1b was spread through fractions 11–18. The IC74 was found to be part of the 20S DHC1a species, but it did not cosediment with the DHC1b. Anti-1b immunoreactive protein was present in fractions 11–18, but IC74 was absent from fractions 13–15. A small amount of IC74 was detected in fractions 7–11; this may represent intermediate chain unassociated with any identified heavy chain.

Dynein Sedimentation Patterns Are Affected by Ionic Strength

Testis cytoplasmic dynein, eluted with ATP from Taxol-induced microtubules, was sedimented through 5–20% sucrose gradients made in high ionic strength

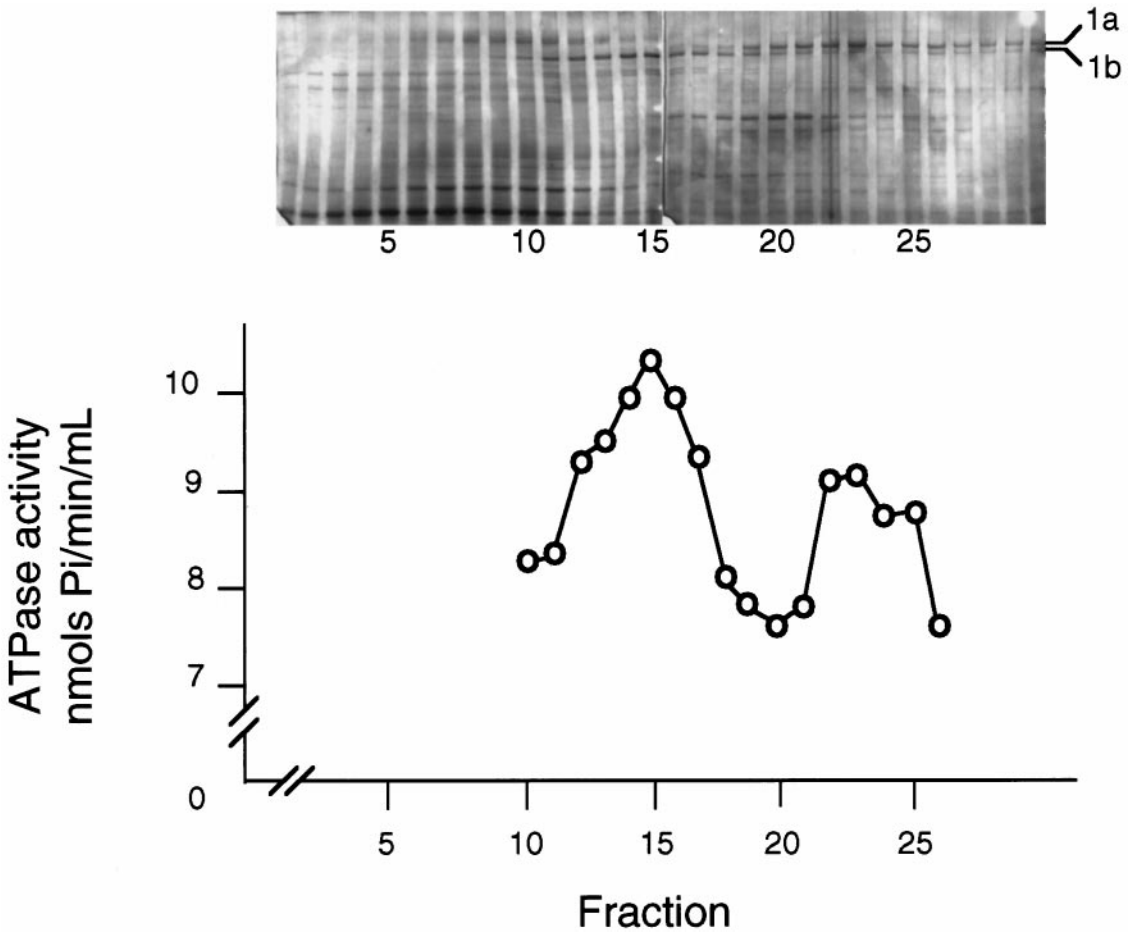

Figure 3. Sucrose density centrifugation of testis cytoplasmic dyneins. The 0.5 M NaCl extract of testis microtubules was sedimented in a linear 5–20% sucrose gradient made in low ionic strength (see MATERIALS AND METHODS), and the gradient was fractionated into 30 equal-volume samples. In separate gradients run in parallel, catalase (11.3S) sedimented in fractions 11–12, and thyroglobulin (19.2S) sedimented in fractions 21–22. Top, silver-stained 6.7% SDS-PAGE of 20 μl of each gradient fraction. The samples were electrophoresed in two identical minigels and are joined together. The positions of DHC1a and anti-1b-immunoreactive protein are indicated. The top of the gradient (fraction 1) is to the left. Bottom, Mg-ATPase activity of each fraction from the same gradient shown in the top panel.

(i.e., wash buffer supplemented with 0.5 M NaCl) and in low ionic strength (i.e., wash buffer with no added salt). The sedimentation patterns of HMr proteins are shown in Figure 5. In the high-ionic-strength gradient, the DHC1a sedimented near the middle of the gradient (approximately 16S) and the DHC1b sedimented at approximately 14S. In contrast, in the low-ionic strength gradient, the DHC1a sedimented faster (approximately 20S) and the DHC1b was spread through a greater region of the gradient (Figure 5, fractions 11–18). This result is similar to the one illustrated in Figure 3 in which the sample was extracted from the microtubules with 0.5 M NaCl instead of ATP.

Further Characterization of the Antibodies

In our previous study, competitive binding experiments indicated that the anti-1a antiserum was not completely peptide-specific because it partially cross-reacted with the 1b peptide and DHC1b protein (Criswell *et al.*, 1996). This prompted us to attempt to obtain cleaner patterns in the Western blots. We affinity purified the antibodies and established two levels of stringency for washing the blots, as described in MATERIALS AND METHODS. Using the high-stringency conditions, the reactivity of each of the affinity-purified antibodies could be completely eliminated by preabsorption with the appropriate peptide, but the inappropriate peptide had no effect on binding to the dynein heavy chain (Figure 6A).

We then evaluated the sucrose gradient fractions with the antibodies. Fractions from ATP-extracted testis cytoplasmic dynein, separated through a low-ionic strength gradient (similar to the one shown in Figure 5), were electrophoresed, blotted, and probed with

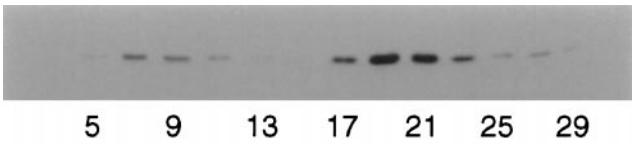

Figure 4. Western blot of dynein intermediate chain IC74 in the sucrose gradient fractions. The odd-numbered fractions (3–29) from a sucrose gradient were resolved on an 8% SDS-polyacrylamide gel and blotted to nitrocellulose. In this gradient, DHC1a was present in fractions 17–23, with its highest concentration in fractions 19–21, and DHC1b was present in fractions 11–18. The blot was probed with anti-IC74, followed by horseradish peroxidase–conjugated secondary antibody and chemiluminescence. The IC74 was associated with DHC1a (fractions 17–23) but did not associate with most of the anti-1b-immunoreactive protein (fractions 11–17).

various antibodies (Figure 6B). At lower stringency, a mixture of the antibodies reacted with the dynein heavy chains throughout the gradient (in this blot, fractions 11–22). The blot was then stripped (see MATERIALS AND METHODS) and reprobed with affinity-purified anti-1a and affinity-purified anti-1b under high-stringency conditions. As expected, DHC1a was confined to the faster sedimenting region of the gradient, in this gradient mostly in fractions 19–21. Unexpectedly, the pattern of anti-1b-immunoreactive proteins changed depending on the stringency conditions of the blotting. At lower stringency, the anti-1b reacted with heavy chains spread through fractions 11–18, a distribution similar to the pattern seen in the silver-stained gel shown in Figure 5. However, under more stringent conditions, the anti-1b reactivity was confined to a narrow region of the gradient, fractions 15–17 in Figure 6B. This result suggests that the anti-1b antibody binds with different affinities to the proteins separated in the gradient.

V1 Photolysis Provides Evidence for Additional 1b-related DHC Isoforms.

The results shown in the gels and Western blots of low-ionic strength sucrose gradients (Figures 3, 5, and 6) suggest that anti-1b-immunoreactive HMr proteins sediment in a broad region of the gradient (fractions 11–18), and that the anti-1b antibody reacts with different affinities to different fractions. To investigate whether these HMr proteins are dyneins, we performed the V1-photolysis reaction on individual sucrose gradient fractions. Cytoplasmic dynein undergoes the V1-photolytic reaction characteristic of all dyneins (Lee-Eiford *et al.*, 1986). This vanadate-mediated photocleavage occurs near the catalytic P1-loop and results in two unequally sized photolytic fragments, called HUV and LUV. Under the conditions used here, the V1-photolysis reaction is diagnostic for dynein.

ATP-eluted cytoplasmic dynein from testis was sedimented through a sucrose gradient made in low-ionic strength buffer. Individual gradient fractions were then subjected to V1 photolysis. The untreated (intact) and V1-photolyzed samples from each gradient fraction were then electrophoresed side by side and the gel was stained with silver. The results are shown in Figure 7. As expected, DHC1a (fractions 19–23 in this gradient) yielded two photolytic frag-

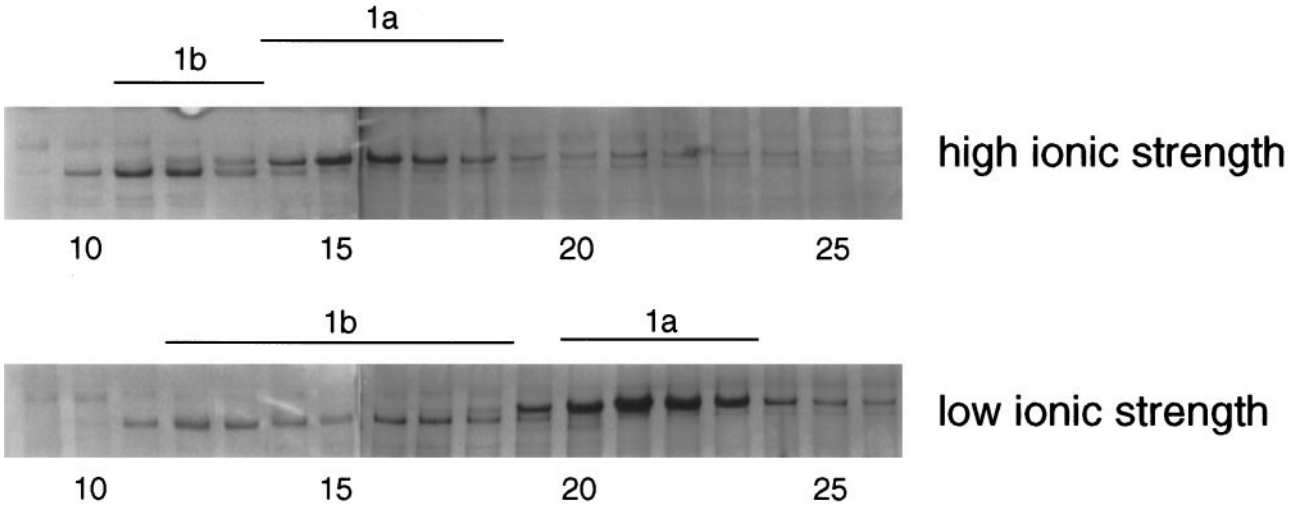

Figure 5. Effect of ionic strength on the sedimentation patterns of cytoplasmic dyneins. Testis cytoplasmic dynein prepared by ATP extraction of microtubules was sedimented in 5–20% sucrose gradients made in high ionic strength (top) or low ionic strength (bottom). The gels of the samples were stained with silver. Each panel shows the DHC regions of two gels joined together. In high ionic strength, the DHC1a sedimented in a peak centered in fractions 15–16, and the anti-1b-immunoreactive protein sedimented in a tight peak centered in fractions 11–12. In low ionic strength, the DHC1a sedimented faster in the gradient, centered in fractions 21–22, and the anti-1b immunoreactive protein sedimented as a broad peak in fractions 11–18.

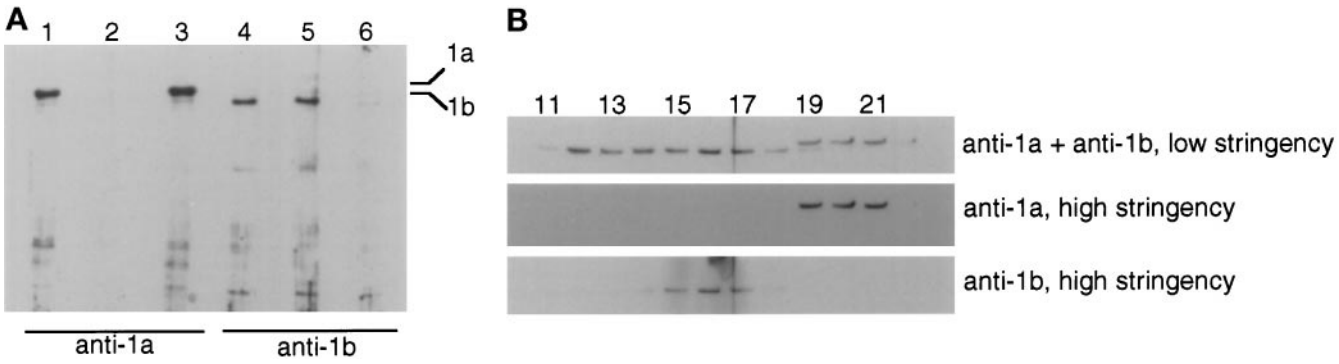

Figure 6. Western blot analysis of sucrose gradient fractions under high-stringency conditions. (A) Western blots using antibodies absorbed with synthetic peptides. Testis cytoplasmic dynein was electrophoresed in 6.7% SDS-polyacrylamide gels, transferred to nitrocellulose, and probed with affinity-purified antibodies that had been preabsorbed with synthetic peptides. The Western blots were processed using the high-stringency conditions (see MATERIALS AND METHODS). Anti-1a antibody: lane 1, no absorption; lane 2, preabsorbed with 1a peptide; lane 3, preabsorbed with 1b peptide. Anti-1b antibody: lane 4, no absorption; lane 5, preabsorbed with 1a peptide; lane 6, preabsorbed with 1b peptide. Under these conditions, the antibodies reacted with the appropriate heavy chain wholly in a sequence-specific manner. (B) Western blots of sucrose gradient fractions. Selected fractions of a low-ionic strength sucrose gradient similar to the one shown in Figure 5 were electrophoresed, blotted, and probed with antibodies. The same blot was repeatedly stripped and reprobed. The heavy chain regions of the blots are shown. Top, anti-1b at low stringency, to which anti-1a was added. Middle, anti-1a at high stringency. Bottom, anti-1b at high stringency. The anti-1b antibody reacted only with a subset of the 1b-like proteins present in fractions 11–17 (see Figure 5).

ments (open symbols). However, a total of six distinct photolytic fragments were produced by fractions 11–17; these products are marked with filled symbols. The pattern of photolytic products changed through the gradient. The slowest sedimenting protein (fraction 11) gave rise to two photolysis products, the largest HUV and the smallest LUV. Fraction 12 gave rise to the two larger HUVs and the two smaller LUVs. Fractions 13–15 gave rise to all six products. Fraction 16 gave rise to four products, but in a different pattern than that of fraction 12; fraction 16 produced the largest and smallest HUVs, and the smallest and largest LUVs. Finally, fraction 17 gave rise predominantly to the smallest HUV and the largest LUV. The pattern of photolysis products allowed us to pair each HUV with an LUV: the largest HUV with the smallest LUV; the middle HUV with the middle LUV; and the smallest HUV with the largest LUV. The pairings are summa-

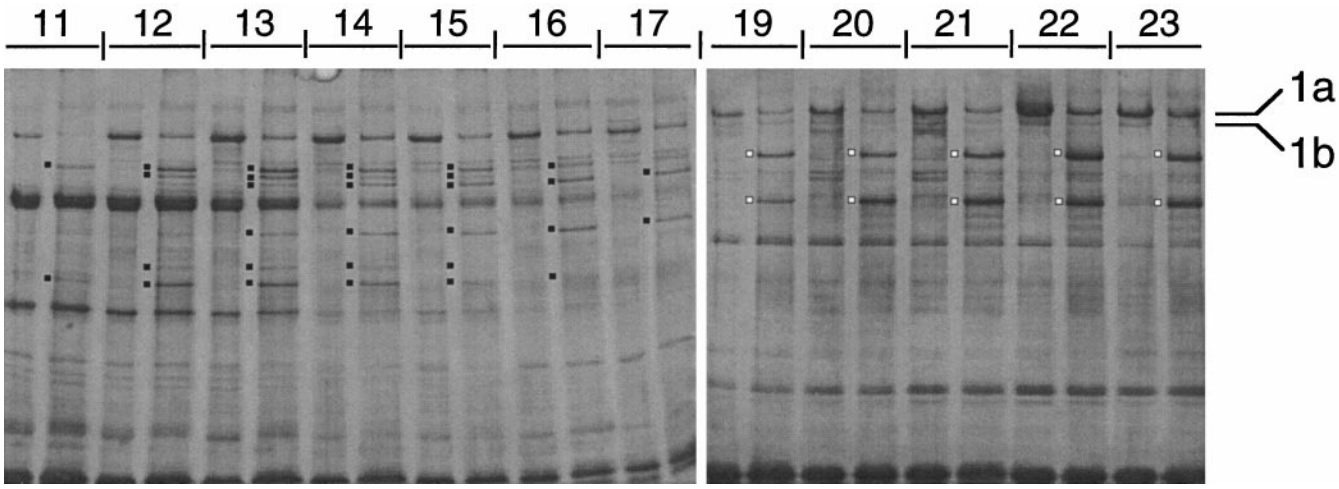

Figure 7. V1 photolysis of cytoplasmic dynein heavy chains separated in a sucrose gradient. Testis cytoplasmic dynein prepared by ATP extraction of microtubules was sedimented through a 5–20% sucrose gradient made in low ionic strength. One hundred-microliter aliquots of individual gradient fractions 11–17 and 19–23 were subjected to V1 photolysis. Equal volumes of untreated and V1-photolyzed samples were resolved in 6.7% SDS-polyacrylamide gels and stained with silver. Two gels were joined together. The principal V1-photolytic products are marked with dots. The 1b-like fractions (11–17) yielded six V1-photolytic products (filled dots). The pattern of products changed through the gradient. DHC1a (fractions 19–23) yielded two V1-photolytic products (open dots).

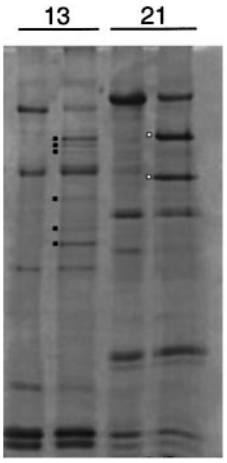

Figure 8. V1-photolysis products of cytoplasmic dynein heavy chains. The untreated and V1-photolyzed fractions 13 and 21 from the gradient shown in Figure 7 were electrophoresed side by side. The principal V1-photolytic products are indicated by dots.

rized in Figure 9A. In other experiments, similar results were obtained with 0.5 M NaCl extracts from testis sedimented in low-ionic strength gradients. These results indicate that the HMr proteins identified in fractions 11–17 are dynein heavy chains, as determined by their susceptibility to V1 photolysis.

To more accurately compare the photolysis patterns of the 1b and 1a regions of the gradient, selected samples were electrophoresed side by side in the same gel. As shown in Figure 8, the six photolysis products from fraction 13 are distinct from the two products from fraction 21. The DHC1a HUV (fraction 21) electrophoreses slightly slower than the largest HUV in fraction 13.

The Previously Cloned DHC1b (DHC2) Gene Product Is One of the Three Slower Sedimenting Dyneins

The results shown in Figure 6B suggested that the anti-1b antibody reacted better with a portion of the gradient fractions, the faster sedimenting 1b-like region of the gradient. To investigate the identities of the heavy chains, Western blotting experiments were performed. Figure 9A shows a portion of a silver-stained gel with intact and V1-photolyzed samples from the 1b region of a low-ionic strength gradient. The six photolysis products are numbered to indicate the pairs of products. A similar gel was then blotted to nitrocellulose and probed with antibodies. As shown in Figure 9B, the pan-reactive JR antiserum reacted with the parent heavy chains and with the three HUV products, although only weakly with HUV II. Because the epitope for JR is downstream of the V1 site, this is the expected pattern of reactivity. Under high-stringency conditions, our anti-1b antibody stained only the HUV III photolysis product. In addition, the anti-DHC2 (Vaisberg *et al.*, 1996) antiserum, raised against a different portion of the DHC1b, reacted only with the LUV III photolysis product, as would be expected based on the location of the antigenic determinants upstream of the V1 site. In other experiments performed at lower stringency, our anti-1b antibody cross-reacted with all three HUV photolysis products (our unpublished data). On the basis of their sequences, the DHC1b we previously described is identical to the DHC2 characterized by Vaisberg *et al.* (1996). From the results shown here, we conclude that the DHC1b/2 isoform is one of the three dyneins sedimenting in this region of the sucrose gradients, isoform III. The other two dyneins are distinct from DHC1b and are not yet identified, although one may correspond to DHC3 (Vaisberg *et al.*, 1996).

DISCUSSION

In this study, we examined the cytoplasmic dyneins in rat testis. Unlike the brain dyneins, testis cytoplasmic dynein heavy chains appear to differ in molecular weight and can be resolved by SDS-PAGE. The upper band was the same apparent size as brain dynein heavy chain and it reacted with the anti-1a and JR

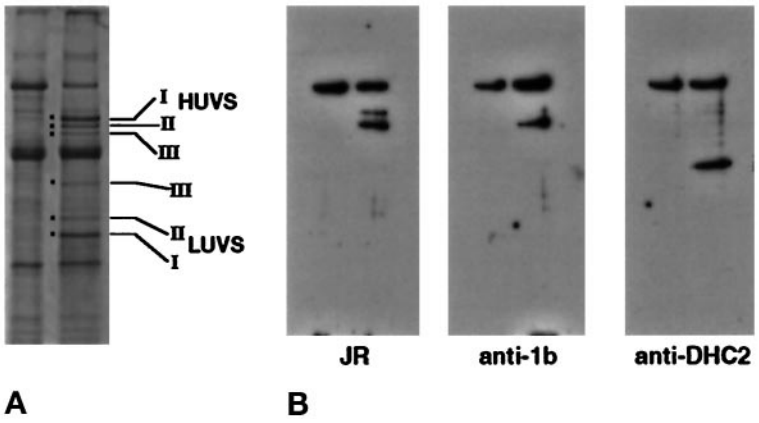

Figure 9. Western blots of intact and V1-photolyzed 1b-like heavy chains. (A) Intact and V1-photolyzed fraction 13 from the gradient shown in Figure 7. The three pairs of HUVs and LUVs are indicated. (B) Western blots of similar samples to those shown in A. The pan-reactive antiserum JR reacted with the parent DHC band as well as the three HUV fragments, although only weakly with HUV II. Anti-1b at high stringency reacted only with the parent DHC band and HUV III. Anti-DHC2 (Vaisberg *et al.*, 1996) at high stringency reacted only with the parent DHC band and LUV III.

antibodies; the lower band reacted with the anti-1b and JR antibodies. This difference in sizes of the proteins was consistent with the slight difference in sizes of the mRNAs as revealed by Northern blots. Furthermore, the deduced sequences of DHC1a and DHC1b from *Caenorhabditis elegans*, the only organism from which there are complete sequences for both heavy chains, indicate that DHC1b is smaller than DHC1a by more than 400 residues (Wilson *et al.*, 1994; Lye *et al.*, 1995).

The two dyneins were separated by sucrose-gradient centrifugation. In low ionic strength, DHC1a sedimented at approximately 20S and the anti-1b-immunoreactive heavy chains sedimented more slowly in a broad band centered at approximately 14S. In high ionic strength, the DHC1a sedimented at approximately 14S and the anti-1b-immunoreactive heavy chains sedimented at approximately 12S. The sedimentation patterns described here are partly similar to the results previously reported with testis cytoplasmic dynein (Collins and Vallee, 1989). In both studies, two peaks of nucleotidase activity–at 20S and 14S–were detected in low ionic strength. However, in our experiments, the slower sedimenting species has a much broader distribution in the gradient. Furthermore, Collins and Vallee (1989) found a major 20S peak of activity in high ionic strength, whereas we found that the DHC1a shifted to a slower sedimenting species in high ionic strength. At present, it is unclear which factors underlie the differences between the two studies. The relatively slow sedimentation of the anti-1b immunoreactive proteins in both high and low salt suggests that these dyneins were isolated as heavy chain monomers.

The Western blot of gradient fractions probed with anti-IC74 indicates that this intermediate chain is mostly associated with DHC1a but not with the DHC1b-like heavy chains. Thus, immunolocalization experiments that rely wholly on anti-IC74 staining may not reveal the full extent of the distribution of cytoplasmic dyneins.

Western blotting of total cytoplasmic dyneins from rat testis indicated that this tissue possesses an unusually high amount (when compared with rat brain) of anti-1b-immunoreactive protein. When testis cytoplasmic dynein was applied to sucrose gradients in low ionic strength, the 1b-like proteins were found to sediment in a broad band in the middle region of the gradient. To evaluate whether these high M_r proteins behaved like dynein, we performed V1-photolysis reactions on individual gradient fractions and determined that all of the heavy chains were indeed susceptible to the same photolysis conditions. However, we were surprised to find that the pattern of photolytic products varied through the 1b portion of the gradient, and we identified three separate cleavage patterns. This finding prompted us to reevaluate the specificity of the antibodies.

The anti-1b antibody was raised against a short synthetic peptide whose sequence distinguishes DHC1b from other dynein heavy chains, including DHC1a and all of the other identified rat axonemal dyneins (Criswell *et al.*, 1996). Previous experiments demonstrated that the anti-1b antibody does not cross-react with 1a protein (Figure 7B in Criswell *et al.*, 1996). At low stringency, the anti-1b antibody reacted with all the gradient fractions containing the 1b-like heavy chains (Figure 6B). The peptide to which the anti-1b antibody was raised is not present in the partial sequences of the characterized rat dynein heavy chains, including the several identified axonemal dyneins (see Figure 1; Tanaka *et al.*, 1995; Andrews *et al.*, 1996; Criswell *et al.*, 1996). At present, we do not know the precise epitope(s) recognized by the antibody, and we do not have the complete sequences of the many different rat dynein heavy chains. Thus, the cross-reaction of the anti-1b antibody with the different heavy chains is intriguing but is not completely understood.

At higher stringency, our anti-1b antibody and anti-DHC2 (Vaisberg *et al.*, 1996) reacted only with the fastest sedimenting 1b-like heavy chain, which gave rise to the HUV-III and LUV-III photolytic products. This is the expected result since the sequences of DHC1b and DHC2 indicate that they are the same gene, and is consistent with the sedimentation pattern of DHC2 from fibroblasts (Vaisberg *et al.*, 1996). We conclude that DHC1b/2 is one of the three heavy chains present in rat testis that are distinguished from DHC1a by their apparently smaller molecular weight and slower sedimentation in sucrose gradients. The finding that the DHC1b gene product is only one of multiple 1b-like proteins is also consistent with the Northern blotting data that indicate that the DHC1b mRNA is lower in abundance than the DHC1a mRNA.

What are the other dynein isoforms identified in this study? Because testis contains spermatozoa, it is possible that these additional isoforms are axonemal dyneins. We view this possibility as unlikely because the dyneins described here partitioned in the soluble fraction after the initial homogenization and centrifugation of the testis, whereas axonemes may be expected to remain insoluble. Furthermore, even if these additional heavy chains are axonemal, it is not obvious why only 2 of the approximately 12 axonemal dyneins would contaminate the cytoplasmic dyneins. On the basis of their slow sedimentation velocities, it is possible that one of the new isoforms identified here corresponds to the DHC3 characterized by Vaisberg *et al.* (1966), although DHC3 does not have the JR-reactive sequence near the P1-loop.

Sucrose gradient centrifugation and V1 photolysis identified four separate cytoplasmic dyneins in rat

testis: DHC1a, DHC1b, and two other isoforms. At low stringency, the two new isoforms reacted with the anti-1b antibody, implying that these heavy chains contain sequences similar to the one to which the anti-1b antibody was raised. At high stringency, only one dynein, DHC1b, reacted with the anti-1b and anti-DHC2 antibodies. This confirms that DHC1b and DHC2 are the same dynein, as is also indicated by their identical sequences where the two clones overlap. The finding that there may exist at least four cytoplasmic dynein heavy chain isoforms in one tissue is consistent with the hypothesis that there are multiple cytoplasmic dyneins to perform different tasks.

ACKNOWLEDGMENTS

We thank Drs. Christine Collins, Jim Forney, and Eugeni Vaisberg for critical discussions of this work, and the reviewers of an earlier version of this article for their helpful comments. We also are grateful to Marlena Thomas, who assisted in the preparation of the figures for this article. Eugeni Vaisberg generously provided us with some of his anti-DHC2 antiserum, which was used in the experiment shown in Figure 9. This work was supported by grants from the American Cancer Society (RPG-96–017-03-CSM) and the National Institutes of Health (GM-49889).

REFERENCES

Amos, L.A. (1989). Brain dynein crossbridges microtubules into bundles. J. Cell Sci. *93*, 19–28.

Andrews, K.K., Nettesheim, P., Asai, D.J., and Ostrowski, L.E. (1996). Identification of seven rat axonemal dynein heavy chain genes: expression during ciliated cell differentiation. Mol. Biol. Cell, *7*, 71–79.

Aniento, F., Emans, N., Griffiths, G., and Gruenberg, J. (1993). Cytoplasmic dynein-dependent vesicular transport from early to late endosomes. J. Cell Biol., *123*, 1373–1387.

Asai, D.J. (1996). Functional and molecular diversity of dynein heavy chains. Semin. Cell Dev. Biol., *7*, 311–320.

Asai, D.J., Beckwith, S.M., Kandl, K.A., Keating, H.H., Tjandra, H., and Forney, J.D. (1994). The dynein genes of *Paramecium tetraurelia*: sequences adjacent to the catalytic P-loop identify cytoplasmic and axonemal heavy chain isoforms. J. Cell Sci., *107*, 839–847.

Asai, D.J., and Brokaw, C.J. (1993). Dynein heavy chain isoforms and axonemal motility. Trends Cell Biol., *3*, 398–402.

Asai, D.J., and Wilson, L. (1985). A latent activity dynein-like cytoplasmic magnesium adenosine triphosphatase. J. Biol. Chem., *260*, 699–702.

Brokaw, C.J. (1994). Control of flagellar bending: a new agenda based on dynein diversity. Cell Motil. Cytoskeleton, *28*, 199–204.

Carter, S.G., and Karl, D.W. (1982). Inorganic phosphate assay with malachite green: an improvement and evaluation. J. Biochem. Biophys. Methods, *7*, 7–13.

Chomczynski, P., and Sacchi, N. (1987). Single-step method of RNA isolation by acid guanidinium thiocyanate-phenol-chloroform extraction. Anal. Biochem., *162*, 156–159.

Cleveland, D.W., and Hoffman, P.N. (1991). Slow axonal transport models come full circle: evidence that microtubule sliding mediates axon elongation and tubulin transport. Cell, *67*, 453–456.

Collins, C.A. (1994). Dynein-based organelle movement. In: Microtubules, ed. J.S. Hyams and C.W. Lloyd, New York: Wiley–Liss, 367–380.

Collins, C.A., and Vallee, R.B. (1989). Preparation of microtubules from rat liver and testis: cytoplasmic dynein is a major microtubule associated protein. Cell Motil. Cytoskeleton, *14*, 491–500.

Corthesy-Theulaz, I., Pauloin, A., and Pfeffer, S.R. (1992). Cytoplasmic dynein participates in the centrosomal localization of the Golgi complex. J. Cell Biol., *118*, 1333–1345.

Criswell, P.S., Ostrowski, L.E., and Asai, D.J. (1996). A novel cytoplasmic dynein heavy chain: expression of DHC1b in mammalian ciliated epithelial cells. J. Cell Sci., *109*, 1891–1898.

Dillman, J.F., III, Dabney, L.P., and Pfister, K.K. (1996). Cytoplasmic dynein is associated with slow axonal transport. Proc. Natl. Acad. Sci. USA, *93*, 141–144.

Dillman, J.F., III, and Pfister, K.K. (1994). Differential phosphorylation in vivo of cytoplasmic dynein associated with anterogradely moving organelles. J. Cell Biol., *127*, 1671–1681.

Dreyfuss, G., Adam, S.A., and Choi, Y.D. (1984). Physical change in cytoplasmic messenger ribonucleoproteins in cells treated with inhibitors of mRNA transcription. Mol. Cell. Biol., *4*, 415–423.

Echeverri, C.J., Paschal, B.M., Vaughan, K.T., and Vallee, R.B. (1996). Molecular characterization of the 50-kD subunit of dynactin reveals function for the complex in chromosome alignment and spindle organization during mitosis. J. Cell Biol., *132*, 617–633.

Eshel, D., Urrestarazu, L.A., Vissers, S., Jauniaux, J.-C., van Vliet-Reedijk, J.C., Planta, R.J., and Gibbons, I.R. (1993). Cytoplasmic dynein is required for normal nuclear segregation in yeast. Proc. Natl. Acad. Sci. USA, *90*, 11172–11176.

Fath, K.R., Trimbur, G.M., and Burgess, D.R. (1994). Molecular motors are differentially distributed on Golgi membranes from polarized epithelial cells. J. Cell Biol., *126*, 661–675.

Gibbons, B.H., Asai, D.J., Tang, W.-J.Y., Hays, T.S., and Gibbons, I.R. (1994). Phylogeny and expression of axonemal and cytoplasmic dynein genes in sea urchins. Mol. Biol. Cell, *5*, 57–70.

Gibbons, I.R. (1995). Dynein family of motor proteins: present status and future questions. Cell Motil. Cytoskeleton, *32*, 136–144.

Hall, E.S., Eveleth, J., Jiang, C., Redenbach, D.M., and Boekelheide, K. (1992). Distribution of the microtubule-dependent motors cytoplasmic dynein and kinesin in rat testis. Biol. Reprod., *46*, 817–828.

Holleran, E.A., Tokito, M.K., Karki, S., and Holzbaur, E.L.F. (1996). Centractin (ARP1) associates with spectrin revealing a potential mechanism to link dynactin to intracellular organelles. J. Cell Biol., *135*, 1815–1829.

Holzbaur, E.L.F., and Vallee, R.B. (1994). Dyneins: molecular structure and cellular function. Annu. Rev. Cell Biol., *10*, 339–372.

Koonce, M.P., and Samso, M. (1996). Overexpression of dynein's globular head causes a collapse of the interphase microtubule network in *Dictyostelium*. Mol. Biol. Cell, *7*, 935–948.

Laemmli, U.K. (1970). Cleavage of structural proteins during the assembly of the head of bacteriophage T4. Nature, *227*, 680–685.

Lee-Eiford, A., Ow, R.A., and Gibbons, I.R. (1986). Specific cleavage of dynein heavy chains by ultraviolet irradiation in the presence of ATP and vanadate. J. Biol. Chem., *261*, 2337–2342.

Li, Y.-Y., Yeh, E., Hays, T., and Bloom, K. (1993). Disruption of mitotic spindle orientation in a yeast dynein mutant. Proc. Natl. Acad. Sci. USA, *90*, 10096–10100.

Lye, R.J., Wilson, R.K., and Waterston, R.H. (1995). Genomic structure of a cytoplasmic dynein heavy chain gene from the nematode *Caenorhabditis elegans*. Cell Motil. Cytoskeleton, *32*, 26–36.

Mazumdar, M., Mikami, A., Gee, M.A., and Vallee, R.B. (1996). In vitro motility from recombinant dynein heavy chain. Proc. Natl. Acad. Sci. USA, *93*, 6552–6556.

Merril, C.R., Goldman, D., Sedman, S.A., and Ebert, M.H. (1981). Ultrasensitive stain for proteins in polyacrylamide gels shows regional variation in cerebrospinal fluid proteins. Science, *211*, 1437–1438.

Mitchell, D.R. (1994). Cell and molecular biology of flagellar dyneins. Int. Rev. Cytol., *155*, 141–180.

Muresan, V., Godek, C.P., Reese, T.S., and Schnapp, B.J. (1996). Plus-end motors override minus-end motors during transport of squid axon vesicles on microtubules. J. Cell Biol., *135*, 383–397.

Neely, M.D., Erickson, H.P., and Boekelheide, K. (1990). HMW-2, the Sertoli cell cytoplasmic dynein from rat testis, is a dimer composed of nearly identical subunits. J. Biol. Chem., *265*, 8691–8698.

Oda, H., Stockert, R.J., Collins, C., Wang, H., Novikoff, P.M., Satir, P., and Wolkoff, A.W. (1995). Interaction of the microtubule cytoskeleton with endocytic vesicles and cytoplasmic dynein in cultured rat hepatocytes. J. Biol. Chem., *270*, 15242–15249.

Pfarr, C.M., Coue, M., Grissom, P.M., Hays, T.S., Porter, M.E., and McIntosh, J.R. (1990). Cytoplasmic dynein is localized to kinetochores during mitosis. Nature, *345*, 263–265.

Piperno, G., and Ramanis, Z. (1991). The proximal portion of *Chlamydomonas* flagella contains a distinct set of inner dynein arms. J. Cell Biol., *112*, 701–709.

Plamann, M., Minke, P.F., Tinsley, J.H., and Bruno, K.S. (1994). Cytoplasmic dynein and actin-related protein arp1 are required for normal nuclear distribution in filamentous fungi. J. Cell Biol., *127*, 139–149.

Porter, M.E. (1996). Axonemal dyneins: assembly, organization, and regulation. Curr. Opin. Cell Biol., *8*, 10–17.

Sale, W.S., and Fox, L.A. (1988). Isolated β-heavy chain subunit of dynein translocates microtubules in vitro. J. Cell Biol., *107*, 1793–1797.

Sambrook, J., Fritsch, E.F., and Maniatis, T. (1989). Molecular Cloning: A Laboratory Manual, 2nd ed., Cold Spring Harbor, NY: Cold Spring Harbor Laboratory.

Satir, P. (1965). Studies on cilia: II. Examination of the distal region of the ciliary shaft and the role of the filaments in motility. J. Cell Biol., *26*, 805–834.

Saunders, W.S., Koshland, D., Eshel, D., Gibbons, I.R., and Hoyt, M.A. (1995). Saccharomyces cerevisiae kinesin- and dynein-related proteins required for anaphase chromosome segregation. J. Cell Biol., *128*, 617–624.

Schnapp, B.J., and Reese, T.S. (1989). Dynein is the motor for retrograde axonal transport of organelles. Proc. Natl. Acad. Sci. USA, *86*, 1548–1552.

Schroer, T.A., Steuer, E.R., and Sheetz, M.P. (1989). Cytoplasmic dynein is a minus end-directed motor for membranous organelles. Cell, *56*, 937–946.

Smith, E.F., and Sale, W.S. (1992). Structural and functional reconstitution of inner dynein arms in *Chlamydomonas* flagellar axonemes. J. Cell Biol., *117*, 573–581.

Steuer, E.R., Wordeman, L., Schroer, T.A., and Sheetz, M.P. (1990). Localization of cytoplasmic dynein to mitotic spindles and kinetochores. Nature, *345*, 266–268.

Summers, K.E., and Gibbons, I.R. (1971). Adenosine triphosphate-induced sliding of tubules in trypsin-treated flagella of sea-urchin sperm. Proc. Natl. Acad. Sci. USA, *68*, 3092–3096.

Tanaka, Y., Zhang, Z., and Hirokawa, N. (1995). Identification and molecular evolution of new dynein-like protein sequences in rat brain. J. Cell Sci., *108*, 1883–1893.

Vaisberg, E.A., Grissom, P.M., and McIntosh, J.R. (1996). Mammalian cells express three distinct dynein heavy chains that are localized to different cytoplasmic organelles. J. Cell Biol., *133*, 831–842.

Vaisberg, E.A., Koonce, M.P., and McIntosh, J.R. (1993). Cytoplasmic dynein plays a role in mammalian mitotic spindle formation. J. Cell Biol, *123*, 849–858.

Vallee, R.B., Wall, J.S., Paschal, B.M., and Shpetner, H.S. (1988). Microtubule-associated protein 1C from brain is a two-headed cytosolic dynein. Nature, *332*, 561–563.

Verde, F., Berrez, J.-M., Antony, C., and Karsenti, E. (1991). Taxol-induced microtubule asters in mitotic extracts of *Xenopus* eggs: requirement for phosphorylated factors and cytoplasmic dynein. J. Cell Biol., *112*, 1177–1187.

Wilson, R., *et al.* (1994). 2.2 Mb of contiguous nucleotide sequence from chromosome III of *C. elegans*. Nature, *368*, 32–38.

Xiang, X., Beckwith, S.M., and Morris, N.R. (1994). Cytoplasmic dynein is involved in nuclear migration in *Aspergillus nidulans*. Proc. Natl. Acad. Sci. USA, *91*, 2100–2104.